LANGMUIR Article
Cite This: Langmuir 2018, 34, 15658−15664
pubs.acs.org/Langmuir

Polyviologen as Electron Transport Material in Photosystem I-Based Biophotovoltaic Cells

Dilek Dervishogullari,[†] Evan A. Gizzie,[†,§] G. Kane Jennings,[‡] and David E. Cliffel*[,†]

[†]Department of Chemistry, and [‡]Department of Chemical and Biomolecular Engineering, Vanderbilt University, Nashville, Tennessee 37235-1822, United States

Supporting Information

ABSTRACT: The photosynthetic protein complex, photosystem I (PSI), can be photoexcited with a quantum efficiency approaching unity and can be integrated into solar energy conversion devices as the photoactive electrode. The incorporation of PSI into conducting polymer frameworks allows for improved conductivity and orientational control in the photoactive layer. Polyviologens are a unique class of organic polycationic polymers that can rapidly accept electrons from a primary donor such as photoexcited PSI and subsequently can donate them to a secondary acceptor. Monomeric viologens, such as methyl viologen, have been widely used as diffusible mediators in wet PSI-based photoelectrochemical cells on the basis of their suitable redox potentials for accepting electrons. Polyviologens possess similar electronic properties to their monomers with the added advantage that they can shuttle electrons in the solid state. Depositing polyviologen directly onto a film of PSI protein results in significant photocurrent enhancement, which confirms its role as an electron-transport material. The polymer film not only improves the photocurrent by aiding the electron transfer but also helps preserve the protein film underneath. The composite polymer−PSI assembly enhances the charge-shuttling processes from individual protein molecules within the PSI multilayer, greatly reducing charge-transfer resistances. The resulting PSI-based solid-state platform demonstrates a much higher photocurrent than the corresponding photoelectrochemical cell built using a similar architecture.

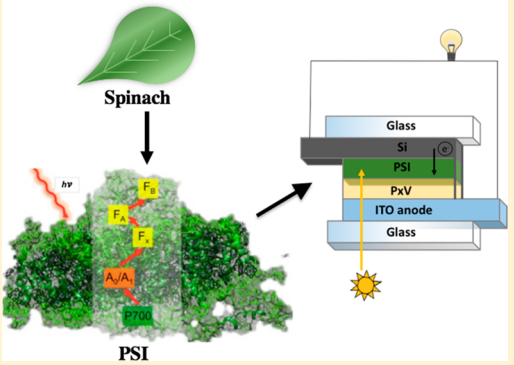

INTRODUCTION

Photosynthesis, the biological conversion of solar energy into chemical energy, is powered by two key proteins, photosystem II (PSII) and photosystem I (PSI), which act in series as biological pseudophotodiodes. Its abundance, ease of extraction, and high internal quantum efficiency have stimulated the integration of PSI in photovoltaic and photoelectrochemical devices. PSI is embedded within the thylakoid membrane, which separates the thylakoid lumen from the stroma. As depicted in Figure 1, following absorption of a photon by the peripheral antenna chlorophylls, a photoexcited electron originates from the P700 reaction center located near the lumenal side of the thylakoid membrane. From P700, the electron is spatially and energetically shuttled through a series of internal cofactors, quickly reaching an iron−sulfur cluster (F_B) located on the stromal side of the protein complex.[1,2] In its native biological environment, the electrons are donated from the reduced F_B^- to the redox protein, ferredoxin, which subsequently feeds adenosine 5′-triphosphate (ATP) and reduced nicotinamide adenine dinucleotide phosphate (NADPH) syntheses in normal plant metabolism as the electron mediator.[3] PSI is highly evolved in its in-vivo role to energetically sustain plant growth and proliferation. However, to fully leverage the efficiency of PSI advantageously in artificial solar energy conversions systems, unique electron

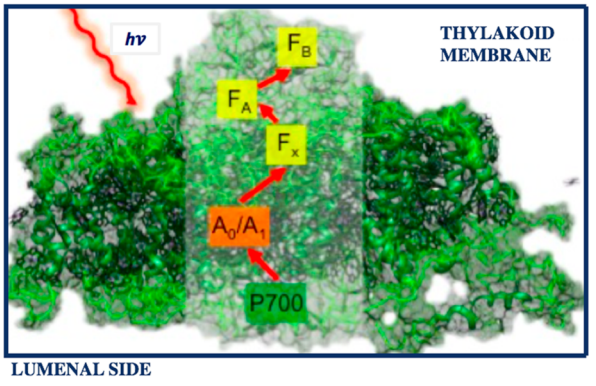

Figure 1. Structure of plant photosystem I protein complex. The image is from PDB entry 2O01 and is modified with the approximate locations of the internal redox mediators.[1,2] PSI is embedded within the thylakoid membrane, which separates the thylakoid lumen from the stroma.

Received: August 31, 2018
Revised: November 28, 2018
Published: November 29, 2018

DOI: 10.1021/acs.langmuir.8b02967
Langmuir 2018, 34, 15658−15664

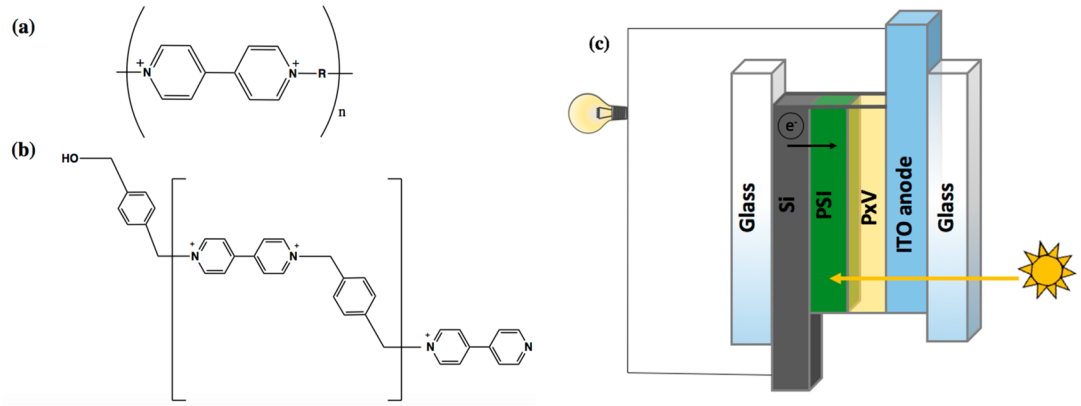

Figure 2. (a) General structure of the polyviologen repeating unit, (b) the structure of a commonly cited polyviologen derivative, poly(*p*-xylylviologen) (PxV), and (c) p-Si/PSI/PxV/ITO solid-state photovoltaic device architecture. Transparent PxV film acts as an electron-transport material between PSI protein and ITO anode.

donor/acceptor materials must be developed and implemented.

Extracted PSI protein has previously been employed as a macromolecular photosensitizer within a host of electrochemical and solid-state photovoltaic architectures. Various electrode materials including metals and semiconductors have been explored for the development of efficient PSI-based solar devices. Semiconductor electrodes provide superior advantages to metal electrodes because of the favorable alignment between energy bands of a carefully chosen semiconductor and PSI. In 2012, LeBlanc et al. demonstrated that the devices derived from multilayer films of PSI deposited onto p-doped silicon (p-Si) substrates outperformed PSI deposited on metallic electrodes such as gold, as well as select semiconductors such as n-type silicon.[4] However, this p-Si/PSI electrode required the use of an electrolyte solution with high concentrations of methyl viologen (MV) mediator.[4] Using a liquid electrolyte with a highly toxic mediator, such as methyl viologen, does not represent a long-term solution. Wet electrochemical cells are not only prone to leaks, but the possible corrosion of the electrodes disrupts the properties of the electrode surface significantly reducing the operational stability and the long-term durability of the electrochemical cell.

Toward the production of scalable photovoltaic devices with long-term operational stability, PSI-based solar energy conversion strategies have begun to focus more on the advancement of solid-state photovoltaics and less on liquid photoelectrochemical cells. In 2007, Carmeli et al. pioneered this effort by preparing PSI films on gold electrodes that retained their photoactivity under dry conditions.[5] A different study in 2014 prepared solid-state biohybrid photovoltaic cells by assembling a monolayer of cyanobacterial PSI onto a TiO_2 substrate and backing the device with a polytriarylamine hole transport layer and an air-sensitive MoO_3/Al cathode.[6] Similarly, in 2015, Beam et al. used ZnO, which was deposited using a pulsed IR laser, as the electron-transport layer between PSI and indium tin oxide (ITO).[7] The resulting solid-state device exhibited significant improvement in photocurrent over a traditional PSI-based photoelectrochemical cell. All of these device architectures were limited by their cost and complicated fabrication methods.

There have been several approaches to utilize solid-state polymer electrolytes and electron/hole transfer materials for overcoming problems associated with liquid electrolytes. Redox polymer-modified electrodes (RPMEs) are increasingly used as electron-transfer catalysts in electrochemical applications.[8] Though RPMEs are most commonly found in biosensors, they display similar electrical properties to conventional semiconductors and thus have a wide range of applications in solar energy conversion when used in conjunction with semiconducting materials. A study by Hamidi et al. demonstrated that immobilized thylakoid membranes on osmium-polymer-modified electrodes generated photoelectrochemical activity, where the osmium redox polymer acted as an electron acceptor from the thylakoid membranes.[9] In 2015, Gizzie et al. incorporated PSI into a polyaniline conductive framework grown directly on TiO_2 electrodes and interfaced this photoactive electrode with an evaporated metallic cathode in order to yield stand-alone solid-state photovoltaics.[10] Both of these studies evidence that the incorporation of PSI into conducting polymer frameworks allows for improved conductivity within the protein−electrode interface. Improving the interfacial electron transfer pathways within PSI multilayers serves a crucial role in achieving higher efficiencies in PSI-based solar devices. Effective electrical wiring of PSI can be achieved through incorporation of PSI in electron-conducting polymer scaffolds.

Polyviologens, first reported in 1971, are a unique class of organic polycationic polymers, with alternating copolymer structure featuring a viologen (*N*,*N*-disubstituted-4,4-bipyridinium dication) and a variable linker group connecting the viologen groups.[11] Aliphatic and unsaturated hydrocarbons of various carbon chain length (e.g., 3−11), as well as aromatic linker groups, have been synthesized and characterized previously.[11−14] A generalized polyviologen structure is presented in Figure 2, along with the structure of a commonly cited polyviologen derivative, poly(*p*-xylylviologen). Although most commonly reported redox polymers involve multistep synthetic routes, polyviologens can be easily synthesized from low-cost precursors in a single step. Polyviologens possess similar electrochemical properties as electron acceptors to their monomeric counterparts that are commonly used as diffusible electrochemical mediators for PSI.

Similar to monomeric viologens, the redox potential of the polymeric viologens can be tuned by alteration of the N-substituted groups attached to the viologen. In polymeric form, these substituent group also serve as linkers between viologen groups in the polymer chain.[11,14] Additionally, polyviologens provide the added advantage of forming robust films because

DOI: 10.1021/acs.langmuir.8b02967
Langmuir 2018, 34, 15658−15664

of their high molecular weights. Importantly, dry films of polyviologens have also demonstrated the ability to shuttle electrons in the solid state.[15] The higher molecular weight contributes to the mechanical stability of the film. Polyviologens are intrinsically redox active (tied to the parent *N*,*N*′-substituted bipyridine) with more positive redox potentials than PSI's final iron−sulfur cluster (F_B). Specifically, the redox potential of poly(*p*-xylylviologen) is −0.196 V versus normal hydrogen electrode (NHE),[15,16] which is energetically lower than the F_B site, making this particular polyviologen derivative ideal for accepting electrons from the reduced iron−sulfur cluster.[4] In addition, the redox potential of the alternating copolymer can be easily tuned by switching the linker groups between the bipyridine moieties.

Polyviologens first attracted attention when Sassoon et al. reported the participation of various polyviologen derivatives in photoinitiated electron-transfer reactions through quenching photoluminescent ruthenium complexes.[17] The quenching behavior confirms that polyviologens rapidly accept excited-state electrons. This was further evidenced by the later observation that photoexcited CdSe quantum dots transfer electrons to poly(*p*-xylylviologen) when two materials are prepared into composite solid-state films.[15,16] Not only does photoelectron transfer from photoluminescent particle to polymer occur on ultrafast time scale (<10 ps), but also the reduced poly(*p*-xylylviologen) is capable of subsequent electron donation to a secondary acceptor such as indium tin oxide (ITO).[15] In the context of interfacing with PSI, Yehezkeli et al. demonstrated a device architecture in which monolayers of PSI were assembled into a film with alternating layers of poly(*p*-xylylviologen) leading to the generation of anodic photocurrents.[18] Although a viable proof of concept, this device required an exogenous, sacrificial electron donor in a liquid electrochemical cell, and the generated photocurrents were only in the nA/cm^2 range.

In the present work, poly(*p*-xylylviologen) (PxV) was used as the electron-transport layer between PSI protein and ITO electrode to construct low-cost, solid-state solar cells. The device architecture is depicted in Figure 2. An aqueous solution of PxV was deposited on multilayer films of PSI protein by vacuum-assisted drop-casting. The thin and transparent nature of the deposited polymer film allows light transmission through the film and light absorption by PSI. The device type that had the polyviologen layer situated between PSI and ITO generated a photocurrent density of 33 μA/cm^2, which is 10 times more than the PSI-only (control) devices and 30 times more than the PxV-only devices. The significant enhancement in anodic photocurrent validates the role of polyviologen in mediating electron transport from PSI to ITO. Effective electrical wiring of PSI multilayer film to the ITO electrode was achieved through incorporation of PSI in an electron-conducting polymer scaffold.

EXPERIMENTAL SECTION

Extraction of Photosystem I Protein Complex. PSI protein was isolated from commercially available organic baby spinach using previously described methods.[19,20] In short, thylakoid membranes were extracted from spinach via maceration, filtration, and centrifugation. The protein was then removed from the membrane and was solubilized using a high concentration of surfactant (Triton X-100) rich media. The protein was purified by hydroxyapatite column and was eluted with 0.2 M sodium phosphate buffer at pH 7. The extracted PSI solution was aliquoted into smaller volumes and was stored at −80 °C. The concentration of the PSI extract was 0.9 × 10^{-6} M as characterized by the methods of Baba et al.[21] Prior to film deposition, excess surfactant and buffer salts in the PSI extract were removed via dialysis against deionized water using regenerated cellulose membrane tubing (molecular weight cut-off (MWCO) 10 kDa).

Synthesis and Characterization of Poly(*p*-xylylviologen). Commercially available reagent-grade chemicals were used without further purification. Poly(*p*-xylylviologen) (PxV) was synthesized by previously reported methods.[12,15,16] Briefly, equimolar amounts of 4,4′-bypyridine and *N*,*N*′-dibromo-*p*-xylene were dissolved in dry acetonitrile in a round-bottom flask capped with an oil-filled bubbler under N_2 atmosphere. The mixture was stirred and heated under reflux at 80 °C for 48 h. The insoluble reaction product was separated from the reaction mixture on a sintered glass vacuum filter (coarse porosity) and was washed with copious amounts of acetonitrile, followed by dichloromethane. The purified yellow solid was dried under low vacuum for 2 h. The product was characterized by voltammetry and ^{1}H NMR. Voltammetry was performed using a CH Instruments 660A workstation. An aqueous 1 mg/mL solution of poly(*p*-xylylviologen) was prepared, was supplemented with 100 mM KCl, and then was argon purged for 30 min to remove any residual oxygen. A 2 mm glassy carbon disk was used as the working electrode, along with a platinum mesh counter electrode and a Ag/AgCl (sat. KCl) reference electrode. Cyclic voltammogram (Figure 4) was collected by scanning from 0 to −0.6 V at a scan rate of 0.01 V/s. The ^{1}H NMR spectrum of the synthesized product is given in Figure S1. From the integrated ^{1}H NMR peaks, the number-average molecular weight (M_n) of poly(*p*-xylylviologen) was estimated to be around 3200 Da, indicating an average of 12 repeating units. Both cyclic voltammetry and ^{1}H NMR data match with previously reported values for poly(*p*-xylylviologen).[15,16]

Modification of Substrates with Photosystem I and Poly(*p*-xylylviologen). Lightly and heavily (boron) p-doped silicon (p-Si) substrates (1−10 Ohm-cm and 0.001−0.005 Ohm-cm, respectively) were purchased from University Wafer (Boston, MA). Each substrate was masked with electrochemical masking tape (Gamry) to yield an exposed area of 1 cm^2. Multilayer films of PSI were deposited onto the unmasked area of the silicon substrates using previously described methods.[4] Briefly, 80 μL of dialyzed PSI solution was pipetted onto the exposed substrate, and a vacuum was applied to remove the solvent. This process yielded multilayer PSI films of approximately 0.4 μm thick. An aqueous 80 μL solution of 10 mg/mL PxV was pipetted onto the dry PSI film, followed by vacuum evaporation. The resulting PSI/PxV film was approximately 0.6 μm thick, indicating that the thickness of the polymer layer was around 0.2 μm. The PSI and polymer film thicknesses were optimized to yield the highest photocurrent. Film thicknesses were determined using a Veeco Dektak 150 stylus profilometer. Profilometer step height from the top of the film to the underlying p-Si was used to determine the average film thickness.

Solid-State Device Fabrication. Solid-state p-Si/PSI/PxV/ITO devices were completed with the addition of an ITO-coated PET anode layer (resistivity: 60 Ω/square, Sigma-Aldrich) on the p-Si/PSI/PxV electrode. To control the exact surface area of the contact, a small piece of transparent PET (0.283 mm^2) was pressed onto the ITO/PET layer, forcing the ITO to contact the PxV surface. For control devices, ITO was contacted on the PSI or bare p-Si surface using the same method. Structural support was provided by sandwiching the entire device stack between two pieces of borosilicate glass (1 mm thickness) and binding the system together with clamps. Detailed fabrication scheme and a picture of the completed device is given in Figure S3.

Electrochemical Measurements. Devices were tested using CH Instruments (Austin, TX) CHI 660a electrochemical workstation. The reference and counter electrode lead wires from the potentiostat were connected to each other and were attached to the ITO anode to form a two-electrode system. The underlying p-Si substrate was connected as the working electrode. Following the determination of the dark open circuit potential (OCP) for each device, this potential was set as the applied voltage during photochronoamperometry

DOI: 10.1021/acs.langmuir.8b02967
Langmuir 2018, 34, 15658−15664

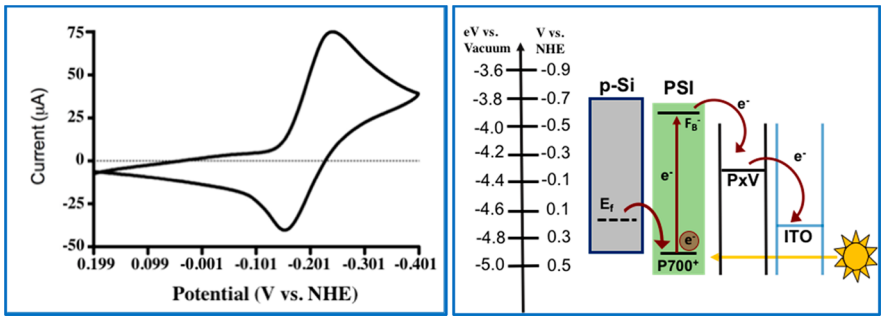

Figure 3. Cyclic voltammogram of the synthesized poly(*p*-xylylviologen) (PxV) (left) and the energy alignment between p-Si, PSI protein, and PxV redox polymer (right).

experiments. During photochronoamperometry experiments, a 10 s period of dark baseline current was first recorded before samples were illuminated through the transparent glass/ITO layer. Illumination was provided by a 250 W cold light source (Leica KL 2500 LCD) generating a light intensity of 0.19 W cm^{-2}. For each chronoamperometry trial, the steady-state photocurrent upon illumination was reported. For liquid photoelectrochemical cells, the PSI-modified silicon substrate was set as the working electrode, Ag/AgCl (sat. KCl) was used as the reference, and platinum mesh wire was used as the counter electrode. The electrolyte solution consisted of 100 mM potassium chloride with 2 mM methyl viologen dichloride hydrate (MV) (Sigma-Aldrich) as the electrochemical mediator.

Absorbance Spectra. UV−vis spectra of PSI and PxV films (Figure S2) were collected using a Varian Cary 5000 UV−vis−NIR spectrophotometer. A background of silicon and borosilicate glass was used to identify only the absorbance contributions of PSI and PxV.

Current Density−Voltage (*j*−*V*) Measurements. Current Density−Voltage (*j*−*V*) curves (Figure 6) for solid-state solar devices were obtained using a SolarTech xenon solar simulator with an AM1.5G filter (class A spectral match, less than 25% mismatch) connected to a Keithley 2400 source meter controlled by a custom Labview program. The lamp was calibrated to 1 sun with a NREL certified photovoltaic standard.

RESULTS AND DISCUSSION

Depositing PSI films onto p-doped silicon (p-Si) results in significant enhancement in photocurrent when compared to metal electrodes such as gold as well as select semiconductors such as n-type silicon. The improved performance of p-Si as a photocathode interfaced with PSI is attributed to the energetic match between the Fermi level of the semiconductor (−4.65 eV vs vacuum) and PSI's oxidized $P700^+$ redox cluster (−4.93 eV vs vacuum).[22] The Fermi level of the p-Si wafers used in this study was calculated from the manufacturer specified resistivity (see Supporting Information part A for the calculation). The small net difference (0.28 eV) between the two energy levels makes the electron transfer from p-Si to $P700^+$ highly energetically favorable. Previous work has demonstrated a dramatic increase in the measured photocurrent of PSI-based systems by using a p-Si substrate in conjunction with a liquid methyl viologen mediator.[4] However, the replacement of the liquid mediator with a solid-state electron-transport material is much more appealing for large-scale practical applications as it increases operational stability in real-world settings. An electron-transport material that has the proper energy alignment with PSI's final iron−sulfur cluster (F_B) is crucial in achieving a good interface between the PSI-modified p-Si and ITO. Polyviologens are intrinsically redox active with higher redox potentials than the F_B site, which makes them ideal for accepting electrons from the cluster.

In this work, a commonly cited polyviologen derivative, poly(*p*-xylylviologen) (PxV), was synthesized by previously reported methods[12,15,16] and was characterized with ^{1}H NMR (Figure S1). Cyclic voltammetry revealed the redox potential ($E_{1/2}$) of $PxV^{2+/1+}$ couple to be −0.196 V versus NHE (Figure 3). The observed potential is in good agreement with previous studies.[15,16] The redox potential of PSI's final iron−sulfur cluster (F_B) sits at around −0.58 V versus NHE.[22] This indicates that the synthesized PxV has a higher redox potential and is energetically lower than F_B and can act as an electron acceptor from the protein on the basis of the favorable energy cascade.

A p-Si/PSI/PxV trilayer biohybrid electrode was designed and fabricated into a solid-state photovoltaic device by placing ITO-coated PET in contact with the PxV layer as an anode. The energy alignment between p-Si, PSI protein, and PxV polymer is shown in Figure 3. Photochronoamperometric analysis revealed that the addition of PxV significantly enhances the generated photocurrent. Figure 4 displays the steady-state photocurrent density comparison of different types of solid-state devices. Thirty replicates of each device type were tested, and the average photocurrent densities along with their corresponding standard deviations (error bars) are presented. In this two-electrode system, the underlying lightly p-doped silicon (p-Si) was connected as the working electrode, and both the reference and the counter electrode connections were attached to the ITO. When the PxV polymer was deposited on

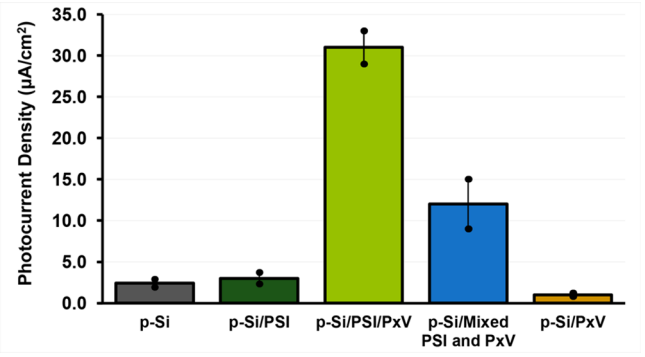

Figure 4. Photocurrent density comparison of solid-state devices. The underlying lightly p-doped silicon (p-Si) is connected as the working electrode, and both the reference and the counter electrode connections were attached to the ITO. The average photocurrent density is calculated from the steady-state current under illumination (n = 30 for each device type). The working electrode is held at the open-circuit voltage in dark.

DOI: 10.1021/acs.langmuir.8b02967
Langmuir 2018, 34, 15658−15664

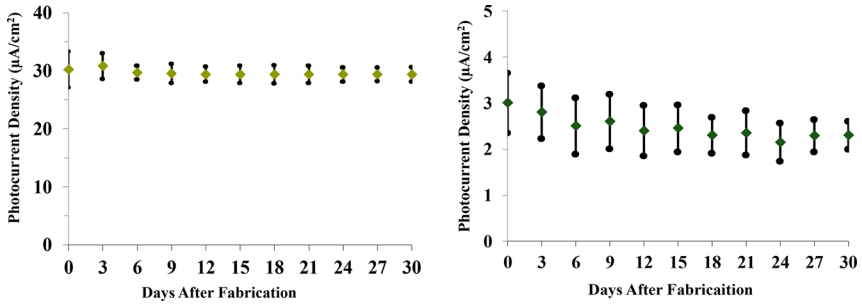

Figure 5. Performance stability of the p-Si/PSI/PxV (left) and p-Si/PSI (right) device types (30 replicates for each type) over 30 days. The underlying p-Si is connected as the working electrode, and both the reference and the counter electrode connections were attached to the ITO. The average photocurrent density is calculated from the steady-state current under illumination.

top of the PSI multilayer film as the electron-transport layer, the best performing device generated a photocurrent density of 33 μA/cm^2. This is 10 times more than the PSI-only control devices and 30 times more than the PxV-only devices. This layered device architecture also outperformed the devices with a mixed PSI protein/PxV polymer composite. These results indicate that the p-Si/PxV electrode is not photoactive by itself and that the transparent PxV film ensures charge transfer between PSI protein and ITO. Overall, the thin (~0.2 μm) PxV film does not interfere with PSI's light absorption; the absorption spectra of deposited thin films of PSI and PxV on glass (Figure S2) show that PxV does not competitively absorb with PSI. PSI absorbs strongly in the red (680 nm) and blue (430 nm) regions, whereas the PxV film absorbs in the green (550 nm) and orange (610 nm) regions.

In addition, p-Si/PSI/PxV devices made with hydrofluoric acid (HF) etched p-Si substrates showed around 3 times higher photocurrent (95 μA/cm^2) than the p-Si/PSI/PxV devices made with unetched p-Si. Although the photocurrent density increased significantly with the removal of the insulating SiO_2 layer through HF treatment, by lowering the internal resistance of the device, a drop (from 250 mV to 210 mV) in the open-circuit voltage (V_{OC}) was also observed. This could be because of the loss of the Schottky barrier in the device. To make sure that the lightly p-doped silicon substrates, which are photoactive by themselves, are not contributing the observed photocurrent in the p-Si/PSI/PxV devices, the same device type replaced the lightly p-doped silicon with heavily p-doped since the heavily p-doped silicon is not photoactive by itself. Although the photocurrents generated from the heavily doped p-Si/PSI/PxV devices were lower (by around 4 times), these devices were still photoactive because of the presence and single contribution of PSI protein.

To provide further evidence for PSI-based photoactivity, p-Si/PSI/PxV devices were prepared with inactive PSI protein. Inactive PSI was prepared by heating of the PSI extract to 80 °C. Photochronoamperometry measurements from these devices are presented in Figure S4. The p-Si/PSI/PxV devices made from active PSI generated 30 times more photocurrent density than the devices made with inactive PSI. Absorbance spectra were collected from active and inactive PSI solution in phosphate buffer (pH 7). Inactive PSI does not have the characteristic 680 nm absorption peak that active PSI possesses which indicates that heating denatures the protein and inhibits its photoactive properties. Since biological materials are also prone to environmental damage and degradation, performance stability in biohybrid devices is critical. To analyze the robustness of this novel device type, 30 replicates of the best performing device type (p-Si/PSI/PxV) and the control device type p-Si/PSI were tested over a period of 30 days, and the change in photocurrent density over time was monitored (Figure 5). The error bars represent the deviation from the average photocurrent density for the 30 replicates. The devices were stored in airtight containers in ambient conditions. For the p-Si/PSI/PxV device, there was no significant reduction in performance; the photocurrent density was retained by 97% at the end of the 30-day period, indicating that these devices are suitable for practical applications. The polymer film not only improves the photocurrent generation by aiding the electron transfer but also helps preserve the protein film underneath. PSI-only devices experienced a 20% loss in performance after 30 days.

Current Density−voltage ($j-V$) analysis was used to further evaluate the solid-state solar devices. $j-V$ analyses under both dark and calibrated solar illumination for p-Si/PxV control device and for p-Si/PSI/PxV device are given in Figure 6. The

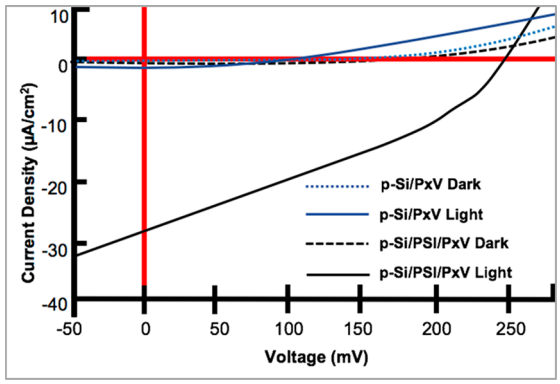

Figure 6. Current Density−voltage ($j-V$) analysis of solid-state p-Si/PSI/PxV (black) and p-Si/PxV (blue) devices. Samples were tested under 1 sun illumination and in the dark.

short-circuit current density (J_{SC}) of the p-Si/PSI/PxV device is 27 μA/cm^2, the open-circuit voltage (V_{OC}) is 250 mV, and the external efficiency is calculated to be 0.0020%. Although the efficiency for the solar cell is low, the simple and inexpensive fabrication method allows for the rapid preparation of a mass number of devices in a low-resource environment. The $j-V$ curves for the same device types made with HF-treated lightly p-doped silicon substrates are given in Figure S5. In the etched p-Si/PSI/PxV device, while the open-circuit voltage (V_{OC}) dropped from 250 mV to 210 mV, the short-circuit current density (J_{SC}) increased from 27 μA/cm^2 to 80

DOI: 10.1021/acs.langmuir.8b02967
Langmuir 2018, 34, 15658−15664

$\mu A/cm^2$. Although the photocurrent density increased significantly with the removal of the insulating SiO_2 layer by lowering the internal resistance of the device, a drop (in the V_{OC}) was also observed. As previously stated, this could be because of the loss of the Schottky barrier in the etched p-Si device.

The calculated external efficiency of the p-Si/PSI/PxV device is higher than the given efficiency (0.0015%) of the previously reported p-Si based PSI device that has a ZnO electron transport layer deposited using confined-plumed chemical deposition. The highest reported external efficiency for a solid-state PSI device (0.0092%) was reported by Gizzie et al. in 2015, who incorporated PSI into a polyaniline conductive framework grown directly on TiO_2 electrodes and who interfaced this photoactive electrode with an evaporated metallic cathode.[10] Our design uses different cathode and anode materials as well as a different conductive polymer network and deposition methods. In addition, our device fabrication methods are simple and low-cost.

In addition to enhancing the photocurrent generation, the incorporation of PxV in solid-state devices changed the shape of the photochronoamperometric curve when compared to a wet-electrochemical cell with a p-Si/PSI electrode and a liquid methyl viologen mediator. Figure 7 displays the photo-

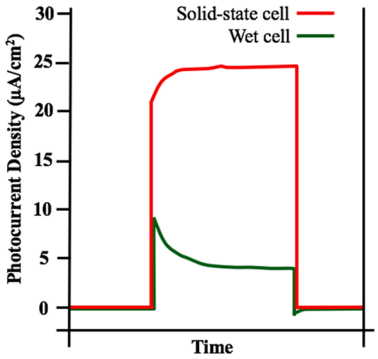

Figure 7. Photochronoamperometric analysis of a solid-state p-Si/PSI/PxV device compared to a liquid photoelectrochemical cell with p-Si/PSI as the working electrode. In the liquid device, the electrolyte consisted of 2 mM methyl viologen and 100 mM KCl, and the counter electrode was Pt mesh. ITO-coated PET was used to make an electrical connection to the PxV layer in the solid-state device, and both the reference and counter electrode connections were connected to the ITO.

chronoamperometry scans from a liquid photoelectrochemical cell and a solid-state p-Si/PSI/PxV device. The liquid cell uses 2 mM methyl viologen mixed with 100 mM KCl as the supporting electrolyte. The cell is connected in a three-electrode system where the p-Si/PSI is wired as the working electrode, Ag/AgCl (sat. KCl) as the reference, and platinum mesh as the counter electrode.

The electrochemical characterization revealed that the solid-state device not only improved the photocurrent density but also changed the shape of the photoamperometric curve. The use of a liquid electrochemical mediator introduced diffusional mass-transfer limitations as indicated by the time decay, while the solid-state device did not have this decay. This pattern follows the Cottrell equation where diffusion-controlled current decays with time. The solid-state devices reach a steady-state photocurrent faster than the wet cells. They also show higher performance stability over time. The improved photocurrent generation in the solid-state device can be attributed to the increased conductivity; the integration of PSI within a conductive PxV polymer framework helps to enhance electron-shuttling processes from individual protein complexes within the multilayer assembly, greatly reducing charge-transfer resistances. As a result, with a smaller number of viologen charge carriers, there is an improved overall charge transfer within the solid-state conductive framework.

CONCLUSION

Polyviologens can be easily synthesized from low-cost precursors and are intrinsically redox active with redox potentials slightly more positive than PSI's final iron−sulfur cluster (F_B), which makes them ideal for accepting electrons from the cluster. Integration of PSI within a conductive polymer framework helps to enhance electron-shuttling processes from individual protein complexes within the multilayer protein film. When the PxV polymer is deposited on top of the PSI multilayer film as the electron-transport layer, the device generated 10 times more photocurrent than the PSI-only control devices and 30 times more photocurrent than the PxV-only devices. The resulting solid-state solar devices showed significant photocurrent enhancement and increased performance stability over a traditional liquid photoelectrochemical cell. The polymer film not only improved the photocurrent generation by aiding the electron transfer but also helped preserve the protein film underneath; PSI-only devices experienced a 20% loss in photocurrent performance after 30 days. This work presents a novel PSI-based solid-state platform for solar energy conversion.

ASSOCIATED CONTENT

Supporting Information

The Supporting Information is available free of charge on the ACS Publications website at DOI: 10.1021/acs.langmuir.8b02967.

Fermi level calculation of p-doped silicon wafers, ^1H NMR characterization of the synthesized poly(*p*-xylylviologen) (PxV), absorbance spectra of PSI and PxV films, schematic for the solid-state device fabrication, inactive PSI absorbance, and photocurrent density performance
(PDF)

AUTHOR INFORMATION

Corresponding Author

*E-mail: d.cliffel@vanderbilt.edu.

ORCID

G. Kane Jennings: 0000-0002-3531-7388
David E. Cliffel: 0000-0001-8756-106X

Present Address

§Northwestern University, 633 Clark St, Evanston, Illinois 60208, United States.

Notes

The authors declare no competing financial interest.

ACKNOWLEDGMENTS

We gratefully acknowledge support from the U.S. Department of Agriculture (2013-67021-21029) and the National Science Foundation (DMR-1507505). Additionally, we acknowledge technical support from the Vanderbilt Institute of Nanoscale

DOI: 10.1021/acs.langmuir.8b02967
Langmuir 2018, 34, 15658−15664

Science and Engineering (VINSE) for use of their instrumentation. Also, we would like to extend special thanks to Kemar R. Reid for assistance in data collection and the Rosenthal Lab at Vanderbilt University for the use of their instrumentation and lab space.

■ ABBREVIATIONS

PSI, photosystem I; ITO, indium tin oxide; PxV, poly(*p*-xylylviologen); polyviologen, PV; MV, methyl viologen dichloride hydrate; p-Si, p-doped silicon; PET, polyethylene terephthalate

■ REFERENCES

(1) Amunts, A.; Drory, O.; Nelson, N. The Structure of a Plant Photosystem I Supercomplex at 3.4Å Resolution. *Nature* **2007**, *447*, 58−63.

(2) Shinkarev, V. P.; Vassiliev, I. R.; Golbeck, J. H. A Kinetic Assessment of the Sequence of Electron Transfer from F_x to F_A and Further to F_B in Photosystem I: The Value of the Equilibrium Constant between F_x and F_A. *Biophys. J.* **2000**, *78*, 363−372.

(3) Hogewoning, S. W.; Wientjes, E.; Douwstra, P.; Trouwborst, G.; van Ieperen, W.; Croce, R.; Harbinson, J. Photosynthetic Quantum Yield Dynamics: From Photosystems to Leaves. *Plant Cell* **2012**, *24*, 1921−1935.

(4) LeBlanc, G.; Chen, G.; Gizzie, E. A.; Jennings, G. K.; Cliffel, D. E. Enhanced Photocurrents of Photosystem I Films on P-Doped Silicon. *Adv. Mater.* **2012**, *24*, 5959−5962.

(5) Carmeli, I.; Frolov, L.; Carmeli, C.; Richter, S. Photovoltaic Activity of Photosystem I Based Self-Assembled Monolayer. *J. Am. Chem. Soc.* **2007**, *129*, 12352−12353.

(6) Gordiichuk, P. I.; Wetzelaer, G. A. H.; Rimmerman, D.; Gruszka, A.; De Vries, J. W.; Saller, M.; Gautier, D. A.; Catarci, S.; Pesce, D.; Richter, S.; Blom, P. W. M.; Herrmann, A. Solid-State Biophotovoltaic Cells Containing PSI. *Adv. Mater.* **2014**, *26*, 4863−4869.

(7) Beam, J. C.; LeBlanc, G.; Gizzie, E. A.; Ivanov, B. L.; Needell, D. R.; Shearer, M. J.; Jennings, G. K.; Lukehart, C. M.; Cliffel, D. E. Construction of a Semiconductor-Biological Interface for Solar Energy Conversion: p-Doped Silicon/Photosystem I/Zinc Oxide. *Langmuir* **2015**, *31*, 10002−10007.

(8) Yuan, Y.; Shin, H.; Kang, C.; Kim, S. Wiring Microbial Biofilms to the Electrode by Osmium Redox Polymer for the Performance Enhancement of Microbial Fuel Cells. *Bioelectrochemistry* **2016**, *108*, 8−12.

(9) Hamidi, H.; Hasan, K.; Emek, S. C.; Dilgin, Y.; Akerlund, H.; Albertsson, P.; Leech, D.; Gorton, L. Photocurrent Generation from Thylakoid Membranes on Osmium-Redox-Polymer-Modified Electrodes. *ChemSusChem* **2015**, *8*, 990−993.

(10) Gizzie, E. A.; Niezgoda, J. S.; Robinson, M. T.; Harris, A. G.; Jennings, G. K.; Rosenthal, S. J.; Cliffel, D. E. Photosystem I-Polyaniline/TiO_2 Solid-State Solar Cells: Simple Devices for Biohybrid Solar Energy Conversion. *Energy Environ. Sci.* **2015**, *8*, 3572−3576.

(11) Factor, A.; Heinsohn, G. E. Polyviologens - a Novel Class of Cationic Polyelectrolyte Redox Polymers. *J. Polym. Sci., Part B: Polym. Lett.* **1971**, *9*, 289−295.

(12) Liu, F.; Yu, X.; Li, S. Preparation of Polyaklylviologen-Polyanion Complexes and Their Applications to the Debromination of Diphenyl Bromomethane Under Heterophase Condition. *J. Polym. Sci., Part A: Polym. Chem.* **1994**, *32*, 1043−1048.

(13) Sassoon, R. E.; Gershuni, S.; Rabani, J. Charge Separation in Photoinitiated Electron-Transfer Systems with Polyviologen Polyelectrolytes as Quenchers. *J. Phys. Chem.* **1985**, *89*, 1937−1945.

(14) Jo, M. Y.; Ha, Y. E.; Kim, J. H. Polyviologen Derivatives as an Interfacial Layer in Polymer Solar Cells. *Sol. Energy Mater. Sol. Cells* **2012**, *107*, 1−8.

(15) Tagliazucchi, M.; Tice, D. B.; Sweeney, C. M.; Morris-Cohen, A. J.; Weiss, E. A. Ligand-Controlled Rates of Photoinduced Electron Transfer in Hybrid CdSe. *ACS Nano* **2011**, *5* (12), 9907−9917.

(16) Tagliazucchi, M.; Amin, V. A.; Schneebeli, S. T.; Stoddart, J. F.; Weiss, E. A. High-Contrast Photopatterning of Photoluminescence within Quantum Dot Films through Degradation of a Charge-Transfer Quencher. *Adv. Mater.* **2012**, *24*, 3617−3621.

(17) Sassoon, R. E.; Gershuni, S.; Rabani, J. Charge Separation in Photoinitiated Electron-Transfer Systems with Polyviologen Polyelectrolytes as Quenchers. *J. Phys. Chem.* **1985**, *89*, 1937−1945.

(18) Yehezkeli, O.; Tel-Vered, R.; Michaeli, D.; Nechushtai, R.; Willner, I. Photosystem I (PSI)/Photosystem II (PSII)-Based Photo-Bioelectrochemical Cells Revealing Directional Generation of Photocurrents. *Small* **2013**, *9* (17), 2970−2978.

(19) Reeves, S. G.; Hall, D. O. [8] Higher Plant Chloroplasts and Grana: General Preparative Procedures (Excluding High Carbon Dioxide Fixation Ability Chloroplasts). *Methods Enzymol.* **1980**, *69*, 85−94.

(20) Ciesielski, P. N.; Faulkner, C. J.; Irwin, M. T.; Gregory, J. M.; Tolk, N. H.; Cliffel, D. E.; Jennings, G. K. Enhanced Photocurrent Production by Photosystem I Multilayer Assemblies. *Adv. Funct. Mater.* **2010**, *20*, 4048−4054.

(21) Baba, K.; Itoh, S.; Hastings, G.; Hoshina, S. Photoinhibition of Photosystem I Electron Transfer Activity in Isolated Photosystem I Preparations with Different Chlorophyll Contents. *Photosynth. Res.* **1996**, *47*, 121−130.

(22) LeBlanc, G.; Chen, G.; Gizzie, E. A.; Jennings, G. K.; Cliffel, D. E. Enhanced Photocurrents of Photosystem I Films on p-Doped Silicon. *Adv. Mater.* **2012**, *24*, 5959−5962.

DOI: 10.1021/acs.langmuir.8b02967
Langmuir 2018, 34, 15658−15664